



Intramolecular electrostatic interactions contribute to phospholipase C β 3 autoinhibition

Candi M. Esquina^{a,1}, Elisabeth E. Garland-Kuntz^{a,b,c}, Daniel Goldfarb^{a,2}, Emily K. McDonald^{c,2}, Brianna N. Hudson^{a,b,c}, Angeline M. Lyon^{a,b,*}

^a The Department of Chemistry, Purdue University, West Lafayette, IN 47906, United States of America

^b The Department of Biological Sciences, Purdue University, West Lafayette, IN 47906, United States of America

^c The Department of Toxicology, Purdue University, West Lafayette, IN 47906, United States of America

ARTICLE INFO

Keywords:

Phospholipase C
Calcium
Phosphatidylinositol lipids
Signaling proteins
Signal transduction
Regulation
Electrostatics

ABSTRACT

Phospholipase C β (PLC β) enzymes regulate second messenger production following the activation of G protein-coupled receptors (GPCRs). Under basal conditions, these enzymes are maintained in an autoinhibited state by multiple elements, including an insertion within the catalytic domain known as the X–Y linker. Although the PLC β X–Y linker is variable in sequence and length, its C-terminus is conserved and features an acidic stretch, followed by a short helix. This helix interacts with residues near the active site, acting as a lid to sterically prevent substrate binding. However, deletions that remove the acidic stretch of the X–Y linker increase basal activity to the same extent as deletion of the entire X–Y linker. Thus, the acidic stretch may be the linchpin in autoinhibition mediated by the X–Y linker. We used site-directed mutagenesis and biochemical assays to investigate the importance of this acidic charge in mediating PLC β 3 autoinhibition. Loss of the acidic charge in the X–Y linker increases basal activity and decreases stability, consistent with loss of autoinhibition. However, introduction of compensatory electrostatic mutations on the surface of the PLC β 3 catalytic domain restore activity to basal levels. Thus, intramolecular electrostatics modulate autoinhibition by the X–Y linker.

1. Introduction

Phospholipase C β (PLC β) enzymes are members of the highly-conserved PLC family, which canonically hydrolyze phosphatidylinositol-4,5-bisphosphate (PIP₂) at the plasma membrane to produce inositol-1,4,5-triphosphate (IP₃) and diacylglycerol (DAG). These second messengers increase intracellular Ca²⁺ and activate protein kinase C (PKC), thereby regulating cell proliferation, differentiation, and survival [4]. PLC β enzymes have low basal activity and are activated through direct interactions with the heterotrimeric G protein subunits G α_q and G $\beta\gamma$, linking PLC β activation to G protein-coupled receptor (GPCR) stimulation [4,5]. The function of PLC β enzymes has been best characterized in the cardiovascular system, where changes in expression and/or G protein-dependent activation contribute to arrhythmias [6,7] and hypertrophy [8].

PLC β shares a highly conserved core domain architecture with other

PLC subfamilies. This core consists of a pleckstrin homology (PH domain), four tandem EF hand repeats, a catalytic TIM barrel domain, and a C2 domain (Fig. 1) [4,9]. These four domains are required for lipase activity in the PLC β subfamily [10]. The PLC β subfamily also contains two C-terminal regulatory domains immediately following the C2 domain. The proximal C-terminal domain (CTD) contains the primary G α_q binding site (H α 1/H α 2) [3] and an autoinhibitory helix (H α 2') [11]. An unconserved linker region connects the proximal CTD to the distal CTD, which contributes to membrane binding and G α_q -dependent activation [12–15].

PLC β is regulated through at least three structural elements, two of which are unique to the PLC β subfamily [11,14,16–18]. The proximal CTD is proposed to stabilize a more catalytically quiescent conformational state [11,18] and inhibit interactions between the core domains and the membrane [19]. The distal CTD also contributes to membrane binding, and may help partition the enzyme between the membrane

Abbreviations: Phospholipase C, PLC; phosphatidylinositol-4,5-bisphosphate, PIP₂; inositol-1,4,5-triphosphate, IP₃; diacylglycerol, DAG; calcium, Ca²⁺; G protein-coupled receptor, GPCR; PE, phosphatidylethanolamine; PIP, phosphatidylinositol phosphate; IP₁, inositol phosphate; differential scanning fluorimetry, DSF.

* Corresponding author at: Depts. of Chemistry and Biological Sciences, Purdue University, 560 Oval Dr., West Lafayette, IN 47907, United States of America.

E-mail address: lyonam@purdue.edu (A.M. Lyon).

¹ Present address: C.M.E.: Albany Molecular Research, Inc., 26 Corporate Circle, Buffalo, New York 12203, United States of America.

² These authors contributed equally.

<https://doi.org/10.1016/j.cellsig.2019.109349>

Received 3 June 2019; Received in revised form 22 June 2019; Accepted 23 June 2019

Available online 26 June 2019

0898-6568/ © 2019 Elsevier Inc. All rights reserved.

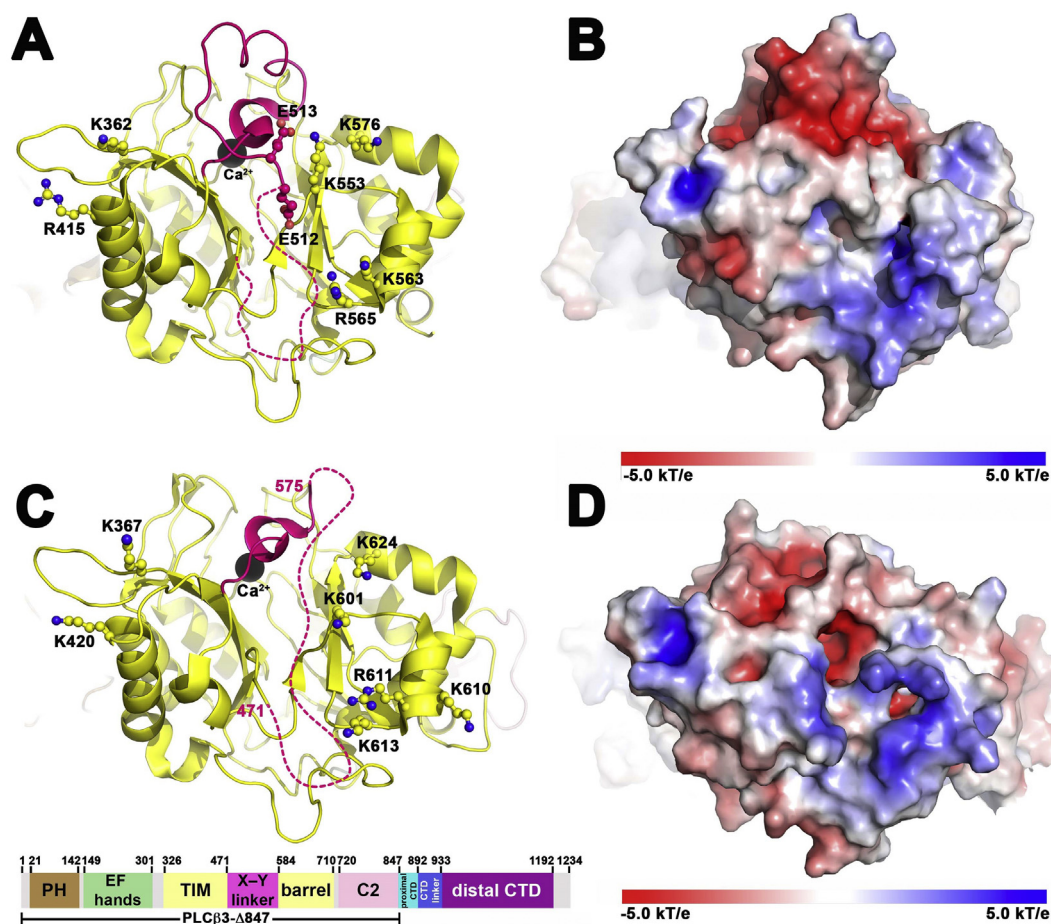


Fig. 1. The PLC β 2 and PLC β 3 X–Y linker and TIM barrel have similar electrostatic properties. (A) A crystal structure of PLC β 2 (PDB ID [2FJU](#) [1]) reveals electron density for the last two residues in the acidic stretch shown in ball and stick (E513 and E512) immediately preceding the lid helix (hot pink). The disordered region of the X–Y linker is shown as a dashed line, with the ends denoted by residue number. The TIM barrel domain (yellow) features highly conserved, solvent-exposed, basic residues (shown in ball and stick). The catalytic Ca $^{2+}$ ion is shown as a black sphere. (B) Electrostatic surface rendering of (A), wherein positive regions are colored blue and negative regions in red [2]. (C) Crystal structure of PLC β 3 (PDB ID [3OJM](#) [3]), shown in the same orientation and coloring as in (A). Shown below the crystal structure is the domain diagram of PLC β 3. Numbers above the diagram corresponds to residues at domain boundaries, and the C-terminal truncation of PLC β 3- Δ 847 is shown below. (D) Electrostatic surface rendering of (C). In both structures, the basic surfaces of the TIM barrel domain could favorably interact with the acidic stretch of the X–Y linker. (For interpretation of the references to colour in this figure legend, the reader is referred to the web version of this article.)

and the cytoplasm [14,19–21]. PLC β is also regulated by the X–Y linker, a variable length insertion within the TIM barrel domain. The X–Y linker is found in several PLC subfamilies, and has been shown to autoinhibit the PLC β , PLC δ , and PLC ϵ subfamilies [4,17]. Deletion of the entire X–Y linker increases basal activity, and in PLC β and PLC ϵ , decreases the efficacy of G protein-dependent activation [17,18]. The proposed mechanism by which regulation by the X–Y linker is achieved is best understood in the context of PLC β . The linker is largely unconserved in length and sequence, with the exception of its C-terminal region which contains a \sim 10–15 stretch of acidic residues followed by \sim 15 residues that fold into a short α helix. This helix interacts with residues adjacent to the active site, functioning as a lid to physically block substrate binding [1,3,11,14,17,18]. Displacement of this lid helix is proposed to occur *via* interfacial activation, wherein unfavorable electrostatic interactions between the acidic stretch of the X–Y linker and the negatively charged membrane leaflet eject the helix to expose the active site [17].

Recent studies suggest the acidic stretch may have multiple roles in interfacial activation. Deletions that include the acidic stretch or deletion of the entire X–Y linker destabilize PLC β to the same extent, suggesting that this region contributes to the global thermal stability of the enzyme. In addition, the crystal structure of a PLC β 3 variant lacking the acidic stretch of the X–Y linker had a disordered lid helix [18]. These

observations suggest that the acidic stretch of the X–Y linker could form stabilizing interactions with the surface of the PLC β core, fixing the lid helix in the bound conformation observed in most crystal structures [1,3,11,14,17,18]. In support of this hypothesis, a prior crystal structure of PLC β 2 revealed electron density for the last two residues of the acidic stretch that appear to interact with conserved basic residues on the surface of the TIM barrel domain [1]. These electrostatic interactions between the disordered acidic stretch and basic residues on the lipase domain could be sufficient for lid helix stabilization, thereby increasing thermal stability and inhibiting basal activity. Indeed, conserved basic residues on the surface of the TIM barrel are also observed in structures of PLC β 3 (Fig. 1) [1,3,11,14,17,18].

Prior studies have tried to dissect the function of the X–Y linker through deletion analysis. Herein, we sought to refine analysis of the linker by creating charge reversal mutants in human PLC β 3 to test hypotheses concerning the molecular mechanisms underlying auto-regulation by the linker. For these studies, we used a C-terminal truncation of PLC β 3, PLC β 3- Δ 847 [11,19]. This truncation allows us to directly evaluate the role of surface charge on the catalytic core of the enzyme in basal activity, stability, and liposome binding, without the confounding impact that the membrane binding distal CTD would cause. In addition, this truncation also has robust basal activity due to the removal of the autoinhibitory proximal CTD. We purified PLC β 3-

Δ847 and charge reversal mutants to homogeneity and compared their thermal stabilities, specific activities, and interactions with liposomes. PLC activity has historically been measured using a radioactivity-based liposome assay *in vitro*. However, the radiolabeled [³H]-PIP₂ substrate is no longer commercially available, requiring the development of an alternative approach for measuring activity *in vitro*. We adapted the commercially available IP-One assay, typically used to measure G_q signaling in cells, to measure phosphatidylinositol hydrolysis by PLCβ3 *in vitro*. Using these approaches, we found that reversal of charge in the acidic stretch decreased stability, increased activity, but had no impact on liposome binding. Charge reversal of the basic residues on the predicted membrane-facing surface of the TIM barrel also decreased thermal stability, but had no impact on activity or liposome binding. However, when the charge reversal mutations were combined, lipase activity was restored to wild-type basal levels, despite a marked increase in liposome binding. Taken together, these studies are consistent with a model wherein intramolecular electrostatic interactions between the acidic stretch of the X–Y linker and the PLCβ3 core directly contribute to autoinhibition.

2. Materials and methods

2.1. Cloning, expression, and purification of PLCβ3 variants

PLCβ3 (UniProt entry Q01970), PLCβ3-Δ892, and PLCβ3-Δ847 were cloned, expressed, and purified as previously described [19]. PLCβ3-Δ847 mutants were generated using QuikChange (Stratagene, San Diego, CA) or Q5 site-directed mutagenesis (New England Biolabs, Ipswich, MA). All mutations were sequenced over the open reading frame. PLCβ3-Δ847 charge reversal mutants were expressed and purified as previously described [19]. As an additional control, a charge neutral PLCβ3-Δ847 variant was also generated, wherein the residues of the acidic stretch were mutated to alanine. However, efforts to express and purify this variant to homogeneity were unsuccessful.

2.2. Basal activity assays

PIP₂ hydrolysis by PLCβ3 variants was measured as previously described [19,22]. PLCβ3 was assayed at final concentrations of 2 or 0.5 ng/μL, PLCβ3-Δ892 at 12 ng/μL, and PLCβ3-Δ847 at 4 or 5 ng/μL. All assays were performed at least in duplicate with protein from at least two independent purifications.

PI hydrolysis was measured using a modified version of the commercially available IP-One assay (IP-One G_q Kit, Cisbio, Bedford, MA). 100 μM hen egg white phosphatidylethanolamine and 250 μM soy phosphatidylinositol (Avanti Polar Lipids, Alabaster, AL) were mixed and dried under nitrogen. Lipids were resuspended in sonication buffer (50 mM HEPES pH 7.0, 80 mM KCl, 3 mM EGTA, and 1 mM DTT) and sonicated. Assays contained 50 mM HEPES, pH 7, 80 mM KCl, 16.67 mM NaCl, 0.83 mM MgCl, 3 mM DTT, 1 mg/mL BSA, 2.26 mM free Ca²⁺, and varying amounts of PLCβ3 variant proteins. Protein concentrations were chosen to have activity in the linear range over a 2–10 min time course. The final concentrations used were 20 ng/μL PLCβ3 or PLCβ3-Δ892, 15 ng/μL PLCβ3-Δ847, 0.25 ng/μL PLCβ3-Δ847 E556-566 K, 8 ng/μL PLCβ3-Δ847 K601-624E, 4 ng/μL PLCβ3-Δ847 K367-624E, and 4 ng/μL PLCβ3-Δ847 E556-566 K/K601-624E. Control reactions contained the same components, but lacked CaCl₂. Reactions were initiated by addition of liposomes and transfer to 37 °C. Reactions were quenched upon addition of 5 μL quench buffer (100 mM HEPES pH 7, 160 mM KCl, 1 mM DTT, 210 mM EGTA), and 14 μL of each reaction was then transferred to a 384-well plate (Greiner Bio-One). For IP detection, D₂-labeled IP₁ (fluorescence acceptor) and anti-IP₁ cryptate (fluorescence donor) were pre-incubated with Detection Buffer (Cisbio) and filtered through a 0.2 μm filter (Millipore). 3 μL of D₂-labeled IP₁ and 3 μL anti-IP₁ cryptate were then added to each well used in the 384-well plate. Positive assay controls contained 50 mM HEPES,

pH 7, 80 mM KCl, 16.67 mM NaCl, 0.83 mM MgCl, 3 mM DTT, 1 mg/mL BSA, 2.26 mM free Ca²⁺, D₂-labeled IP₁, and anti-IP₁ cryptate, while negative assay controls contained all components except D₂-labeled IP₁. The plate was then incubated for 1 h in the dark at room temperature, followed by centrifugation at 1000 ×g for 1 min. Plates were read with a Synergy 4 plate reader (BioTek) at 620 and 665 nm. IP₁ was quantified using a standard curve and data reduction protocol for normalization (Cisbio). Data were plotted and statistics were performed using GraphPad Prism v8.0.

2.3. Differential scanning fluorimetry

Thermal stability of PLCβ3-Δ847 and mutants was determined as previously described [19]. Samples contained 0.2–0.5 mg/mL of the PLCβ3-Δ847 mutant plus 5 mM CaCl₂. All experiments were performed in triplicate from at least two independent protein preparations. Thermal denaturation curves were fit to a Boltzman sigmoidal function, and the T_m was calculated from the inflection point (GraphPad Prism 8.0).

2.4. Liposome binding assays

PLCβ3-Δ847 variant binding to PE:PIP₂ liposomes was performed as previously described [23], with some modifications. Briefly, 200 μM hen egg white phosphatidylethanolamine and 100 μM porcine brain phosphatidylinositol 4,5-bisphosphate (Avanti Polar Lipids) was mixed and dried under N₂. Lipids were resuspended in 312 μL sonication buffer (50 mM HEPES, pH 7, 80 mM KCl, 3 mM EGTA, and 1 mM DTT), and sonicated. 125 pmol of each PLCβ3-Δ847 variant was incubated with 65 μL of PE:PIP₂ liposomes and sonication buffer in a final volume of 100 μL. Control samples contained protein and buffer only. Samples were incubated for 1 h on ice, then centrifuged at 119,000 ×g for 1 h at 4 °C. The supernatant was transferred to a 1.7 mL microfuge tube, the remaining pellet was resuspended in 100 μL sonication buffer, and all samples were stored on ice. 16 μL of the supernatant or resuspended pellet was then denatured with 4 μL of 5 × SDS loading dye, and 5 μL of this total sample analyzed by SDS-PAGE. All gels were stained with Bio-Safe Coomassie (Bio-Rad), and band density was quantified with ImageJ and normalized to controls. Each variant was examined at least three times from two different protein preparations.

2.5. Statistical methods

All graphical plots were generated using GraphPad Prism v.8.0. One-way ANOVA was performed with Prism 8.0 and followed by Tukey post-hoc multiple comparisons as noted in figure captions. Error bars represent standard deviation.

3. Results

3.1. Charge reversal mutations in the X–Y linker and the TIM barrel decrease thermal stability

If the acidic stretch in the linker interacts with basic patches on the TIM barrel domain, then the thermal stability of the protein would be expected to decrease when the interaction is disrupted, such as by the introduction of charge reversal mutations. To test this hypothesis, site-directed mutations were introduced in the background of PLCβ3-Δ847, a C-terminal truncation of PLCβ3 that has been previously used to investigate autoinhibition and lacks the regulatory proximal and distal CTDs that would confound analysis (Fig. 1). First, the eleven aspartic and glutamic acid residues in the acidic stretch were all converted to lysine to create PLCβ3-Δ847 E556-566K (Table 1), and its thermal stability compared to that of PLCβ3-Δ847 using differential scanning fluorimetry.

(DSF) [24]. PLCβ3-Δ847 (referred to as WT) had a melting

Table 1
PLC β 3- Δ 847 Charge Reversal Mutations.

Variant	Mutation
PLC β 3- Δ 847	<i>H. sapiens</i> PLC β 3 residues 10-847
E556-566K	E556K/D557K/E558K/E559K/E560K/D561K/E562K/E563K/E564K/E565K/E566K
K601-624E	K601E/K611E/R613E/K624E
K367-624E	K367E/K420E/K601E/K610E/K611E/R613E/K624E
E556-566K/K601-624E	E556K/D557K/E558K/E559K/E560K/D561K/E562K/E563K/E564K/E565K/E566K/ K601E/K611E/R613E/K624E

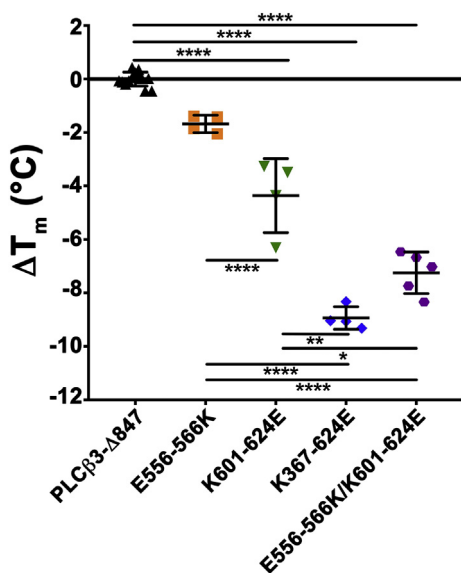


Fig. 2. Differential scanning fluorimetry (DSF) was used to measure the T_m of each PLC β 3- Δ 847 charge reversal variant. Mutations within the X-Y linker and/or the TIM barrel domain decrease the T_m of each variant (ΔT_m) relative to PLC β 3- Δ 847. Data represent at least two independent experiments measured in triplicate \pm SD, from at least two purifications. Significance was determined by one-way ANOVA followed by Tukey's multiple comparison test (****, $p \leq .0001$; **, $p \leq .0024$; *, $p \leq .0113$).

Table 2
Thermal Stability and Basal Activity of PLC β 3- Δ 847 Charge Reversal Mutants.

PLC β 3- Δ 847 variant	$T_m \pm$ SD ($^{\circ}$ C)	Specific Activity \pm SD (nmol IP $_1$ /min/nmol enzyme)
PLC β 3- Δ 847 (WT)	54.6 \pm 0.3 ^a	0.14 \pm 0.03
E556-566K	53.3 \pm 0.6 ^b	8.9 \pm 2.3 ^c
K601-624E	48.9 \pm 2.4 ^{c,d}	0.11 \pm 0.1
K367-624E	45.7 \pm 0.4	0.016 \pm 0.009
E556-566K/K601-624E	46.5 \pm 1.6	0.19 \pm 0.08

Data represent at least three independent experiments measured in duplicate \pm SD, from at least two protein purifications. Significance was determined by one-way ANOVA followed by Tukey's multiple comparison test.

^a $p \leq 0.0001$, relative to all mutants except PLC β 3- Δ 847 E556-566K.

^b $p \leq 0.0001$, relative to K601-624E and K367-624E, E556-566K/K601-624E.

^c $p \leq 0.0024$ relative to K367-624E.

^d $p \leq 0.0113$ relative to E556-566K/K601-624E.

^e $p \leq 0.0001$ relative to all other mutants.

temperature (T_m) of 54.6 \pm 0.3 $^{\circ}$ C, while the T_m of PLC β 3- Δ 847 E556-566K was decreased to 53.3 \pm 0.6 $^{\circ}$ C (Fig. 2, Table 2).

The surface of the TIM barrel domain features conserved, basic residues predicted to be in close proximity to the acidic stretch of the X-Y linker (Fig. 1) [1,3]. To determine whether these basic residues contribute to thermal stability, two charge reversal mutations were generated. PLC β 3- Δ 847 K601-624E and PLC β 3- Δ 847 K367-624E (Table 1),

convert four or seven residues to glutamates, respectively, that are in close proximity to the C-terminus of the X-Y linker acidic stretch based on crystal structures (Fig. 1A, C) [1,3]. While all of these residues are solvent-exposed, two (K420 and R611) also form electrostatic interactions with acidic residues in close proximity, thereby contributing to the tertiary structure of the TIM barrel. However, both variants were properly folded as assessed by size exclusion chromatography, demonstrating the mutations do not compromise the structure. We found that PLC β 3- Δ 847 K601-624E had a T_m of 48.9 \pm 2.4 $^{\circ}$ C, \sim 6 $^{\circ}$ C lower than WT. PLC β 3- Δ 847 K367-624E was further destabilized, with a T_m of 45.7 \pm 0.4 $^{\circ}$ C, \sim 9 $^{\circ}$ C lower than WT (Fig. 2, Table 2). If the loss of thermal stability reflects a loss of favorable electrostatic interactions between the linker and the TIM barrel, then charge reversal mutations in both the acidic stretch and the TIM barrel domain (PLC β 3- Δ 847 E556-566K/K601-624E, Table 1) should restore stability. However, this variant had a T_m of 46.5 \pm 1.6 $^{\circ}$ C. Thus, even a variant with the combined charge reversal mutation was destabilized \sim 7 $^{\circ}$ C relative to WT (Fig. 2, Table 2).

3.2. PLC β 3 variants hydrolyze PIP $_2$ and PI *in vitro*

The gold-standard assay for measuring *in vitro* PLC β basal activity has been a liposome-based activity assay, wherein [3 H]-PIP $_2$ is incorporated into liposomes. Following incubation with enzyme, free [3 H]-IP $_3$ is quantified by scintillation counting [22]. However, this critical radiolabelled substrate is no longer commercially available, necessitating the development of an alternative assay for measuring *in vitro* PLC β activity. PLC enzymes are known to hydrolyze other phosphatidylinositols, including PI, albeit with reduced specific activity [25]. Thus, we turned to the IP-One assay (CisBio, Bedford, MA), which is a well-established method for measuring IP $_1$ accumulation in cells following stimulation of G $_q$ -coupled receptors. This assay relies on homogenous time resolved fluorescence (HTRF), wherein the fluorescent donor and acceptor interact and emit baseline fluorescence. Upon PIP $_2$ hydrolysis, IP $_3$ is produced and is rapidly degraded to IP $_1$. As IP $_1$ accumulates in the cell, it binds the fluorescent donor, displacing the acceptor and decreasing the total fluorescence [26,27].

We expressed and purified full-length PLC β 3 and two previously characterized C-terminal truncations, PLC β 3- Δ 847 and PLC β 3- Δ 892, and compared their ability to hydrolyze [3 H]-PIP $_2$ versus PI using *in vitro* liposome-based activity assays. [3 H]-PIP $_2$ hydrolysis was measured using well-established protocols [18,19,22]. For PI hydrolysis, PI was incorporated into liposomes with phosphatidylethanolamine (PE), using an analogous method as the PIP $_2$ hydrolysis assay [18,19,22]. In both assays, PLC β 3 variants were incubated with the substrate liposomes for increasing times in the presence of \sim 200 nM free Ca $^{2+}$, while control assays lacked Ca $^{2+}$ [22]. [3 H]-IP $_3$ was quantified by scintillation counting, whereas *in vitro* IP accumulation was measured by monitoring the change in fluorescence as a function of time, with the final concentration of IP quantified using a standard curve [26,27]. All three PLC β 3 variants were able to hydrolyze [3 H]-PIP $_2$ or PI under the experimental conditions (Fig. 3). Full-length PLC β 3 has the highest activity with both substrates, compared to PLC β 3- Δ 892, consistent with the presence of the distal CTD [5]. When PIP $_2$ is the substrate, PLC β 3 has a specific activity of 37.1 \pm 10.5 nmol IP $_3$ /min/nmol enzyme, similar to previous reports [11], versus 0.14 \pm 0.05 nmol IP $_1$ /min/nmol

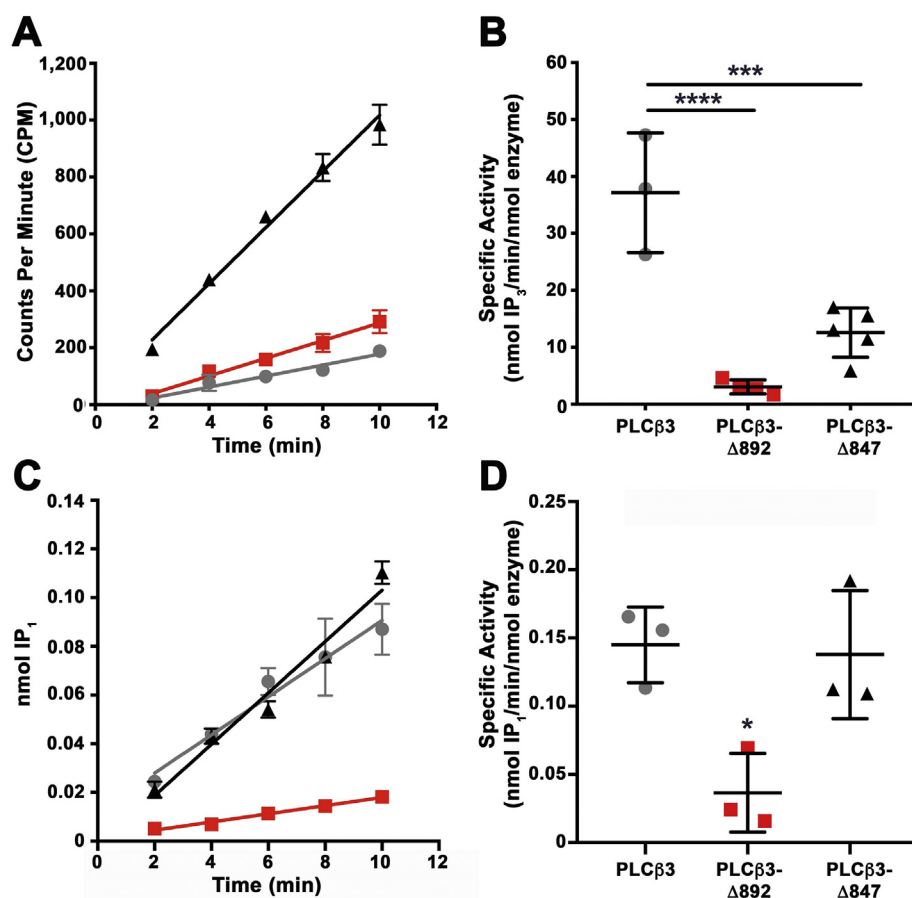


Fig. 3. PLCβ3 variants hydrolyze PIP₂ and PI from liposomes. (A) The ability of PLCβ3 (gray circles), PLCβ3-Δ892 (red squares), and PLCβ3-Δ847 (black triangles) to hydrolyze [³H]-PIP₂ from liposomes was measured as a function of time. (B) The specific activity of PLCβ3 is 37.1 ± 10.5 nmol IP₃/min/nmol enzyme, PLCβ3-Δ892 is 3.0 ± 1.2 nmol IP₃/min/nmol enzyme, and PLCβ3-Δ847 is 13 ± 4.3 nmol IP₃/min/nmol enzyme (****, *p* < .0001, ***, *p* ≤ .0007). (C) The ability of PLCβ3 (gray circles), PLCβ3-Δ892 (red squares), and PLCβ3-Δ847 (black triangles) to hydrolyze PI from liposomes was also measured as a function of time. (D) The specific activity of PLCβ3 is 0.14 ± 0.05 nmol IP₁/min/nmol enzyme, PLCβ3-Δ892 is 0.04 ± 0.03 nmol IP₁/min/nmol enzyme, and PLCβ3-Δ847 is 0.14 ± 0.03 nmol IP₁/min/nmol enzyme (*, *p* < .03). Data represents the average from at least three independent experiments in duplicate ± SD. Significance was determined by one-way ANOVA followed by Tukey's multiple comparison test. (For interpretation of the references to colour in this figure legend, the reader is referred to the web version of this article.)

enzyme when PI is the substrate. PLCβ3-Δ847 has significantly higher basal activity than PLCβ3-Δ892 whether PIP₂ or PI is used as the substrate (Fig. 3) [11,18]. Finally, the specific activity of PLCβ3-Δ892 is decreased ~4-fold when PI is the substrate, compared to PIP₂ (Fig. 3). Although the PLCβ3 variant specific activities are decreased with the PI substrate, the IP-One assay is a viable approach for measuring for measuring PLCβ3 activity *in vitro*.

3.3. Charge reversal mutations modulate basal activity

Prior reports suggest that destabilization may contribute to activation of PLCβ [18]. To determine whether destabilization caused by the charge reversal mutations similarly releases autoinhibition, the basal activity of all PLCβ3-Δ847 variants was measured using PI hydrolysis. PLCβ3-Δ847 had a specific activity of 0.14 ± 0.03 nmol IP₁/min/nmol enzyme (Fig. 4, Table 2). The specific activity of PLCβ3-Δ847 E556-566K was 8.9 ± 2.3 nmol IP₁/min/nmol enzyme, a ~64-fold increase compared to WT PLCβ3-Δ847, and consistent with the acidic stretch being required for autoinhibition. This is comparable to the reported ~30-fold increase in lipase activity when the entire X-Y linker was deleted in PLCβ3-Δ847 [18].

In contrast, mutation of the basic TIM barrel surface (PLCβ3-Δ847 K601-624E and PLCβ3-Δ847 K367-624E) had no significant impact on basal activity. Combining the charge reversal mutants in PLCβ3-Δ847 E556-566K/K601-624E also resulted in specific activity similar to the WT protein (Fig. 4, Table 2). As mutations to the TIM barrel decrease activity and thermal stability, it may be that the electrostatic properties of this domain are critical for normal function.

3.4. PLCβ3-Δ847 charge reversal variants have altered liposome binding

PLCβ3 must associate with the cell membrane in order to hydrolyze

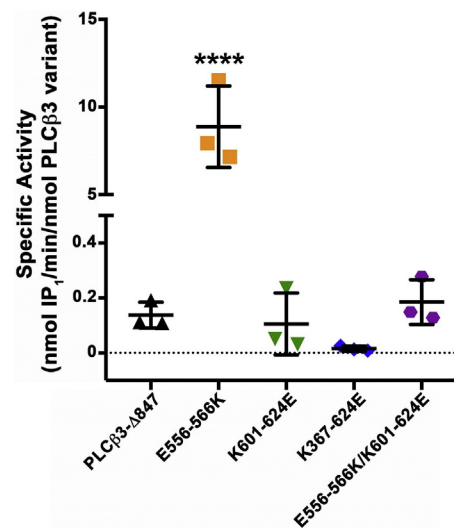


Fig. 4. Mutation of the acidic stretch in the X-Y linker increases enzyme activity. PLCβ3-Δ847 (black triangles) hydrolyzes PI from liposomes with a specific activity of 0.14 ± 0.03 nmol IP₁/min/nmol enzyme. Charge reversal of the X-Y linker in PLCβ3-Δ847 E556-566K (orange squares) significantly increases basal activity (****, *p* < .0001). Mutation of the TIM barrel in K601-624E (green inverted triangles) and K367-624E (blue diamonds) has minimal impact on activity. Combining the charge reversal mutations in E556-566K/K601-624E (purple hexagons) does not alter basal activity. Data represents the average from at least three independent experiments in duplicate ± SD. Significance was determined by one-way ANOVA followed by Tukey's multiple comparison test. (For interpretation of the references to colour in this figure legend, the reader is referred to the web version of this article.)

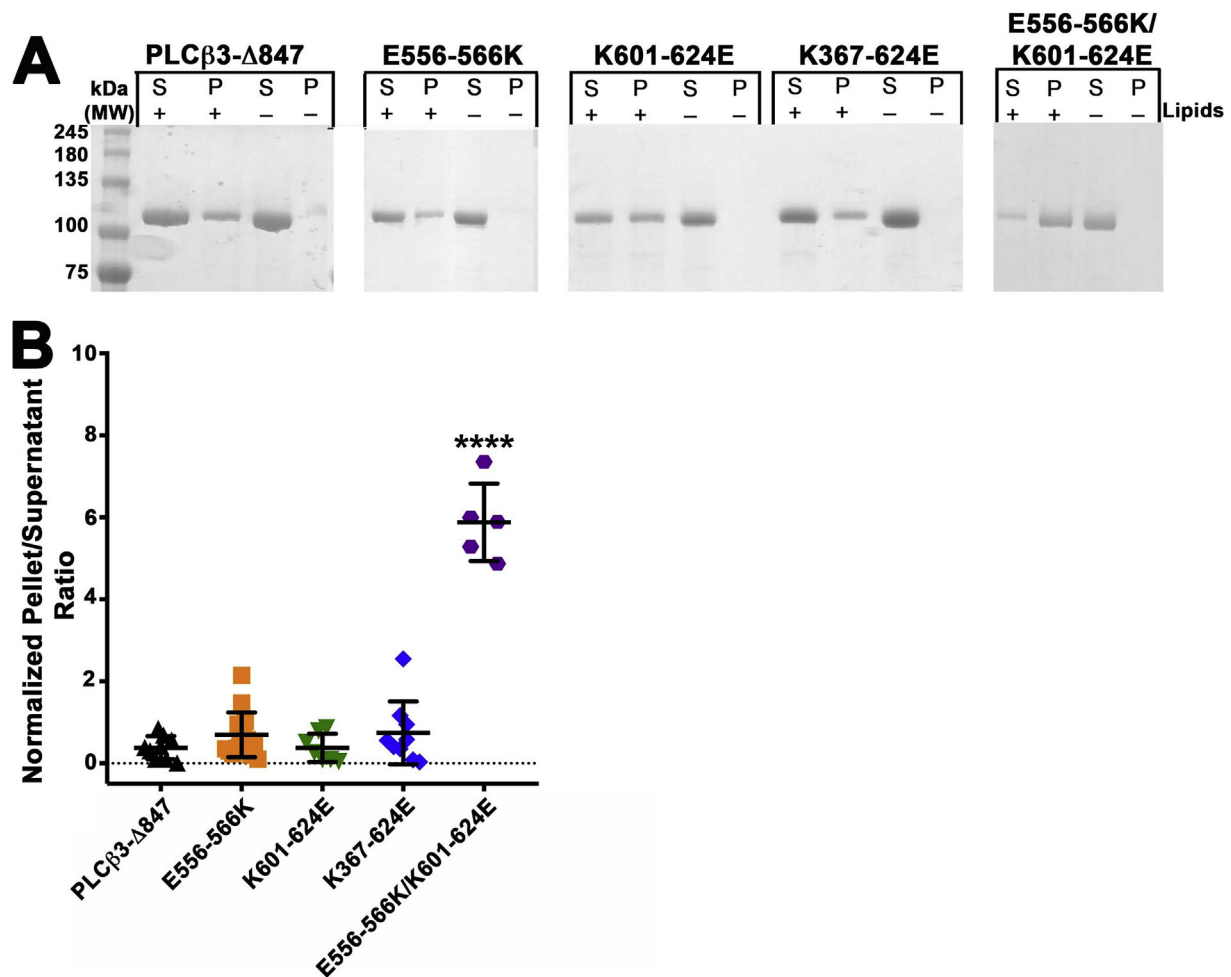


Fig. 5. Charge reversal of the acidic stretch within the X–Y linker and the basic residues on the TIM barrel increase liposome binding. (A) Representative SDS-PAGE gels of PLCβ3-Δ847 and charge reversal variants after incubation with (+) PE:PIP₂ liposomes or (–) buffer. Identical volumes of supernatant (S) or resuspended pellet (P) were analyzed for each experiment. White spaces show samples analyzed on different gels. (B) The band density of the pellet and supernatant fractions under each condition were quantified using ImageJ. PLCβ3-Δ847 and charge reversal mutants are present primarily in the supernatant following incubation with liposomes, with the exception of the PLCβ3-Δ847 variant, E556-566A/K601-624E, which is present in the pellet after incubation. Data represent at least three independent experiments ± SD. Significance was determined by one-way ANOVA followed by Tukey's multiple comparison test (****, $p \leq .0001$).

its substrate, and alteration of the electrostatic surface perturbs activity and stability. To investigate whether these mutations also perturb the ability of the enzyme to bind to liposomes, a pull-down assay was used to monitor the binding of the PLCβ3-Δ847 variants to PE:PIP₂ liposomes [23,28]. PLCβ3-Δ847 lacks the distal CTD, which is required for maximum membrane binding, and thus would be expected to bind only weakly to PE:PIP₂ liposomes. As expected, the majority of this protein is present in the supernatant fraction following incubation with PE:PIP₂ liposomes. There is a band present in the pellet fraction, consistent with modest liposome binding and the low basal activity of this variant (Fig. 5) [4,12,19]. Similarly, mutation of the acidic stretch to polylysine in PLCβ3-Δ847 E556-566K had no impact on liposome binding, with the majority of the protein present in the supernatant. Thus, the increased basal activity of this variant is not due to increased interactions with liposomes (Fig. 5).

The ability of the PLCβ3-Δ847 TIM barrel charge reversal mutants to bind the PE:PIP₂ liposomes was then tested. While the basic residues on the TIM barrel surface are not anticipated to contribute to liposome binding, as evidenced by these variants having basal activity comparable to WT, the primary membrane binding surface of PLCβ3 has not yet been experimentally validated [18,19]. PLCβ3-Δ847 K601-624E and PLCβ3-Δ847 K367-624E were both found primarily in the supernatant after incubation with liposomes (Fig. 5), confirming these basic

surfaces are not directly involved in liposome binding.

Lastly, PLCβ3-Δ847 E556-566K/K601-624E was assessed for its ability to bind liposomes. Surprisingly, this mutant was found predominantly in the pellet after incubation with liposomes. This result cannot be attributed to charge reversal of the X–Y linker, as PLCβ3-Δ847 E556-566K interacted with liposomes to a similar extent as PLCβ3-Δ847 (Fig. 5). This increased binding also cannot be due to increased interactions between the active site and the liposome, as PLCβ3-Δ847 E556-566K/K601-624E has basal activity comparable to WT (Table 2). These results suggest that introduction of compensatory acidic mutations to the TIM barrel surface, in the presence of the basic X–Y linker, are sufficient to decrease basal activity independently of liposome binding.

4. Discussion

The poorly conserved X–Y linker is one of the most studied auto-inhibitory elements in PLCβ [10,16–18], but little is known about its mechanism, other than the fact that deletion of the acidic stretch or the entire linker is activating. This has been proposed to be due to elimination of unfavorable charge-charge interactions between the linker and the membrane, which increase substrate binding to the active site [16,17]. However, crystallization of a PLCβ3 mutant containing a

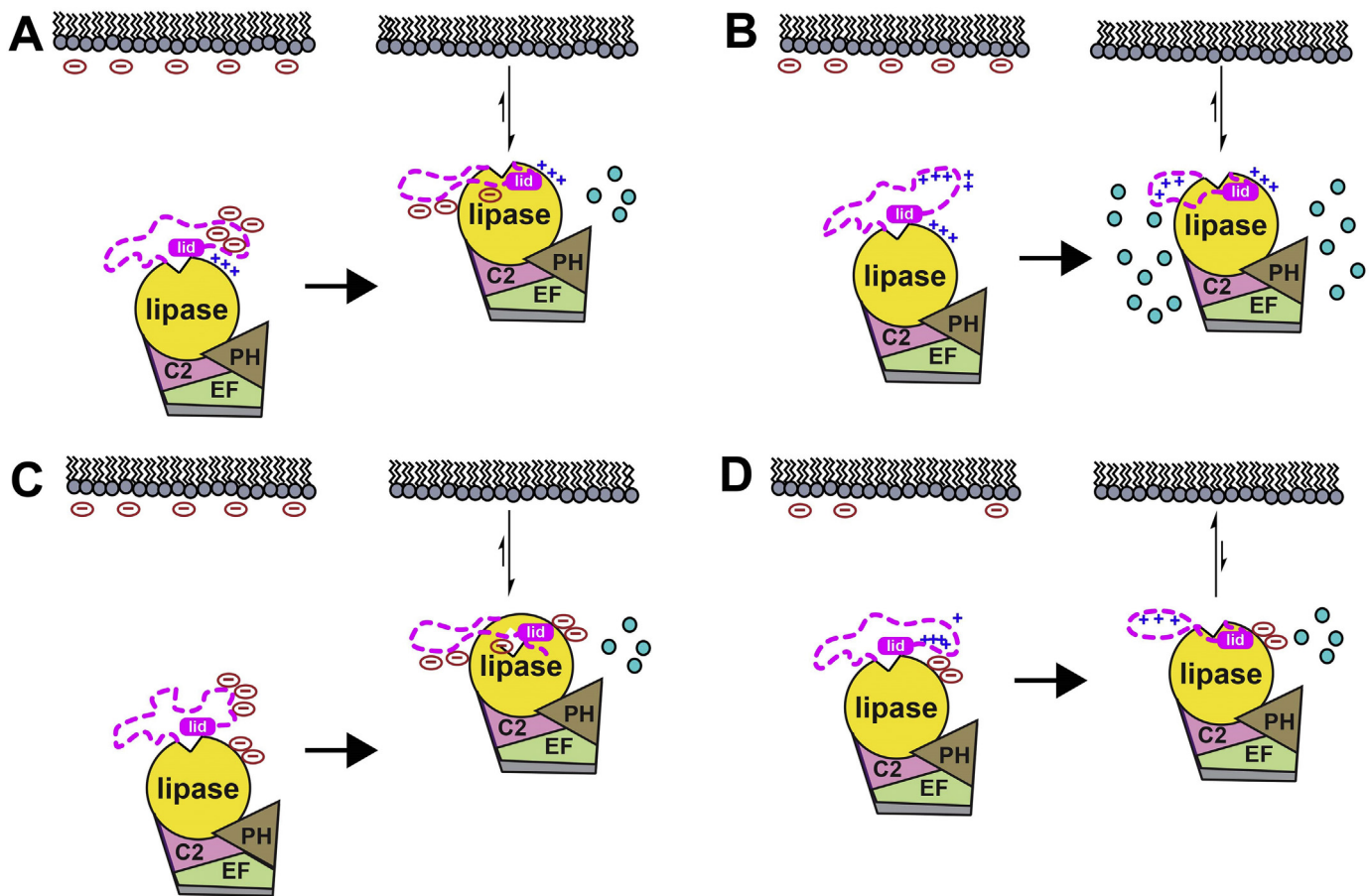


Fig. 6. Intramolecular electrostatic interactions modulate PLC β 3 activity. The electrostatic properties of the X–Y linker and the TIM barrel contribute to activity, stability, and liposome binding. Domains are colored as in Fig. 1, with teal circles representing IP $_3$ produced upon PIP $_2$ hydrolysis. (A) In the wild-type enzyme, the acidic stretch of the X–Y linker (circled minus signs) hinders membrane binding (right). Interfacial activation displaces the acidic stretch and lid helix, allowing the active site to bind the negatively charged membrane (circled minus signs), potentially aided by the basic surface of the TIM barrel (blue plus signs) (left). (B) Reversing the charge of the acidic stretch to polylysine (right) increases basal activity without altering liposome binding (left). (C) Reversing the charge of the acidic stretch to polylysine (right) increases basal activity without altering liposome binding (left). (D) Reversing the charge of the acidic stretch and the TIM barrel decreases stability (right) and increases liposome binding, but has no impact on basal activity (left). In this mutant, the X–Y linker could interact with the membrane and/or the TIM barrel. (For interpretation of the references to colour in this figure legend, the reader is referred to the web version of this article.)

deletion of the acidic stretch revealed that the lid helix becomes disordered in the absence of the acidic stretch [18], suggesting that this region may interact with the TIM barrel to stabilize the conformation of the lid that blocks access to the active site. This indicated that interfacial activation is more complex than simple modulation of charge–charge interactions.

In this work, site-directed mutagenesis was used to investigate whether electrostatic interactions between the X–Y linker and the catalytic TIM barrel domain contribute to PLC β 3 regulation. Mutation of the acidic stretch to polylysine (PLC β 3- Δ 847 E556-566K) did not alter thermal stability relative to PLC β 3- Δ 847, suggesting that regions of the linker that flank the acidic stretch are important for maintaining stability (Fig. 2, Table 2). However, this mutation increased basal activity ~60-fold without appearing to increase binding to negatively charged liposomes (Figs. 4, 5, Table 2). The latter is surprising given the activity of this mutant and the more complementary charge of the linker with the liposome. One possible explanation is that PIP $_2$ was depleted from the liposome over the time course of the experiment (1 h), decreasing the negative charge of the liposome and therefore binding [19,21]. We then introduced charge reversal mutations on the surface of the TIM barrel domain (PLC β 3- Δ 847 K637-624E and PLC β 3- Δ 847 K601-624E). These variants had decreased stability, but no significant change in activity or association with liposomes (Figs. 2, 4, 5). The PLC β 3 crystal

structure (PDB ID 3OHM [3]), reveals that K420 and R611 form electrostatic interactions with E373 and E616, respectively, within the TIM barrel. Disruption of interactions such as these may contribute to the ~5–7 °C decrease in stability of these variants. In addition, introduction of negatively charged residues on the TIM barrel surface also introduces unfavorable electrostatic interactions with the membrane, leading to reduced activity even if the X–Y linker has been displaced (Figs. 1, 2, Table 2). In support of these ideas, the charge-swapped mutant, PLC β 3- Δ 847 E556-566K/K601-624E, was less stable than PLC β 3- Δ 847, but as predicted, had comparable basal activity (Figs. 2, 4, 5, Table 2). Surprisingly, this was the only variant that strongly bound to liposomes (Fig. 5).

Overall, these studies emphasize that membrane binding does not always correlate with activity in this system. PLC β 3- Δ 847 variants containing charge reversal mutations on the TIM barrel domain all have decreased thermal stability. Furthermore, with the exception of the combined charge reversal mutant (PLC β 3- Δ 847 E556-566K/K601-624E), they did not bind liposomes. These trends may have a dominant effect on activity independently of whether the lid helix of the X–Y linker is bound near the active site or not. Overall, the presence of a net negative charge, whether in the acidic stretch of the X–Y linker or on the surface of the TIM barrel is detrimental. However, these results paint a mixed picture as to whether or not interactions between the X–Y

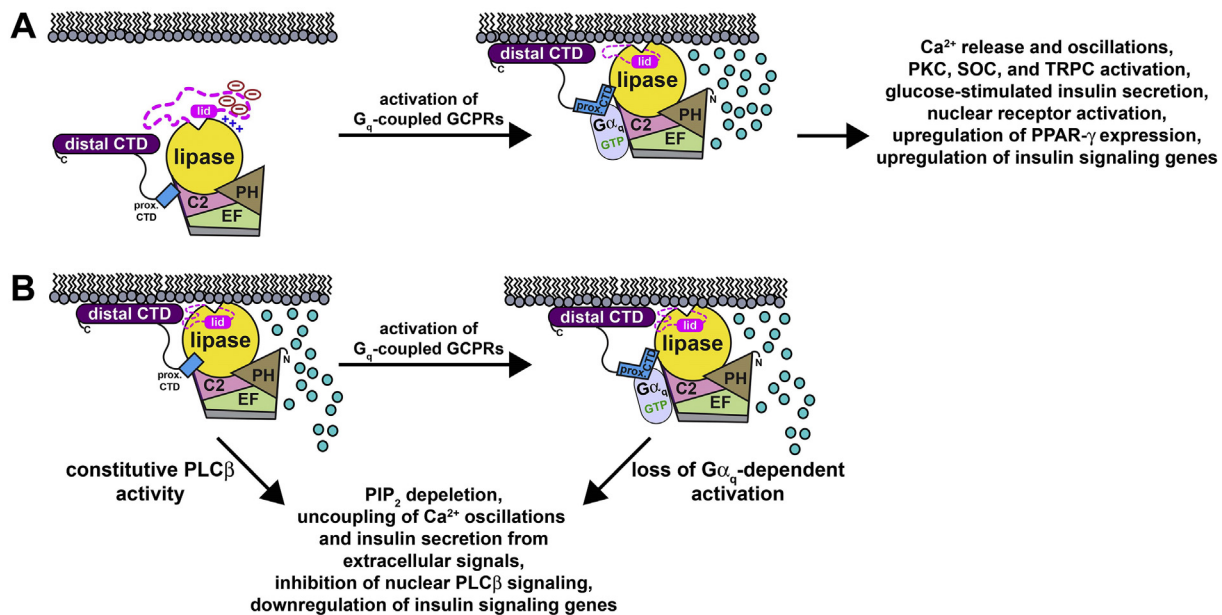


Fig. 7. Potential roles for PLC β activity in pancreatic β -cells. Domains are colored as in Fig. 1, with teal circles representing IP $_3$ produced upon PIP $_2$ hydrolysis. (A) Following the stimulation of G $_q$ -coupled GPCRs, G α_q binds to PLC β , stimulating its lipase activity. The increase in the second messengers IP $_3$ and DAG activating downstream events required for normal insulin secretion, including the induction of Ca $^{2+}$ oscillations, ion channel activation, and nuclear signaling events such as upregulation of PPAR- γ . (B) Electrostatic mutations with PLC β could result in constitutive membrane association and/or activation. While the mutant PLC β 3 could still bind G α_q , the efficacy of activation would be diminished, effectively uncoupling PLC β activity from extracellular signals. This would result in PIP $_2$ depletion, uncoupling and dampening of Ca $^{2+}$ oscillations, decreased nuclear PLC β activity, and downregulation of insulin signaling genes. (For interpretation of the references to colour in this figure legend, the reader is referred to the web version of this article.)

linker and the surface of the PLC β 3 core are responsible for auto-inhibition. Based on our results, it is likely that the membrane, the X-Y linker, and the TIM barrel interact in a more complex way than previously understood that is difficult to deconvolute (Fig. 6). In the future, it would be interesting to look at how X-Y linker charge reversal affects activation by G proteins, and if the TIM barrel charge reversal mutants can still be activated by the G $\beta\gamma$ heterodimer. In addition, the X-Y linker is also found in the PLC δ , PLC ϵ , and PLC ζ subfamilies [17]. In the PLC ζ subfamily, the X-Y linker contains a highly basic region, which is proposed to contribute to membrane binding, consistent with our double charge swapped variant. This basic region was shown to preferentially interact with model membranes containing PIP $_2$ [29]. Thus, it appears that the highly-charged character of the X-Y linker is primarily responsible for regulation mediated by this element. However, further studies are needed to confirm whether the charged nature of the X-Y linker is required for regulation in other subfamilies.

With respect to the charge reversal mutations in PLC β 3 described in this study, perturbation of the electrostatic surfaces on PLC β would be expected to have profound consequences on downstream processes. For example, PLC β has been shown to contribute to glucose-stimulated insulin secretion in pancreatic β -cells [30]. Following activation by G α_q , increased PIP $_2$ hydrolysis by PLC β stimulates intracellular Ca $^{2+}$ release, facilitates opening of store-operated channels (SOC) that conduct Ca $^{2+}$, as well as some transient receptor potential (TRP) channels, such as TRPC3 [31]. In addition to second messenger production at the plasma membrane, PLC β activity in the nucleus is also essential for maintaining normal β -cell function [32–35]. There, PLC β activity upregulates expression of genes involved in insulin secretion, including PPAR- γ (peroxisome proliferator-activated receptor γ) [36,37] (Fig. 7A). Loss of the acidic stretch would be expected to lead to constitutive activity, resulting in depletion of PIP $_2$ and dampening of Ca $^{2+}$ oscillations. Although this mutant would retain the ability to bind activated G α_q , the Ca $^{2+}$ oscillations required for insulin secretion would be uncoupled from extracellular signals. The depletion of PIP $_2$ in the cell would also likely decrease nuclear PLC β activity and the expression

of insulin sensing and secreting genes. Finally, the decrease in PIP $_2$ would also alter other pathways that rely on the balance of phosphatidylinositides in cellular membranes (Fig. 7B) [38].

Finally, this study required the development of a new method for measuring *in vitro* PLC activity. The gold-standard assay in the field has long been the hydrolysis of [3 H]-PIP $_2$ from liposomes [22]. However, this critical reagent is no longer commercially available, and custom biosynthesis of the lipid is prohibitively expensive. To circumvent this problem, we turned to the commercially available IP-One assay, which is routinely used to measure IP accumulation in cells following stimulation of G $_q$ -coupled GPCRs [26,39]. PLC enzymes can hydrolyze other phosphatidylinositol species *in vitro* and in cells [25,40,41], thus PLC-dependent hydrolysis of PI hydrolysis could be detected and quantified. Using human PLC β 3 and two previously characterized C-terminal truncations, we demonstrated that these proteins can hydrolyze PI from liposomes under the same conditions as [3 H]-PIP $_2$ (Fig. 3). These proteins also showed similar trends in specific activity with both substrates (Fig. 3). Thus, the IP-One assay, modified to measure liposome-based PI hydrolysis, is a valid method for measuring *in vitro* PLC activity.

Author contributions

A.M.L. designed the overall experimental approach. C.M.E., E.E.G., D. G. * , and E.K.M. * cloned, expressed, and purified PLC β 3- Δ 847 and all variants. B.N.H. expressed and purified PLC β 3 and PLC β 3 PLC β 3- Δ 892. C.M.E. performed DSF assays, and C.M.E. and E.E.G.-K. performed the activity and liposome binding assays. The manuscript was written through contributions of all authors. All authors have given approval to the final version of the manuscript. * These authors contributed equally.

Funding sources

This work was supported by an NIH 1R01HL141076-01 (A.M.L.), American Heart Association Scientist Development Grant 16SDG29930017 to A.M.L., and an American Cancer Society

Institutional Research Grant (IRG-14-190-56) to the Purdue University Center for Cancer Research (A.M.L.).

Acknowledgement

We thank Osvaldo Cruz-Rodriguez (University of Michigan) for technical assistance with the IP-One assay. This work was supported by an NIH 1R01HL141076-01, American Heart Association Scientist Development Grant 16SDG29930017, and an American Cancer Society Institutional Research Grant (IRG-14-190-56) to the Purdue University Center for Cancer Research (A.M.L.). The content is solely the responsibility of the authors and does not necessarily reflect the official views of the National Heart, Lung, and Blood Institute, or the National Institutes of Health.

References

- [1] M.R. Jezyk, J.T. Snyder, S. Gershberg, D.K. Worthylake, T.K. Harden, J. Sondek, Crystal structure of Rac1 bound to its effector phospholipase C- β , *Nat. Struct. Mol. Biol.* 13 (2006) 1135–1140.
- [2] T.J. Dolinsky, J.E. Nielsen, J.A. McCammon, N.A. Baker, PDB2PQR: an automated pipeline for the setup of Poisson-Boltzmann electrostatics calculations, *Nucleic Acids Res.* 32 (2004) W665–W667.
- [3] G.L. Waldo, T.K. Ricks, S.N. Hicks, M.L. Cheever, T. Kawano, K. Tsuboi, X. Wang, C. Montell, T. Kozasa, J. Sondek, T.K. Harden, Kinetic scaffolding mediated by a phospholipase C- β and G_q signaling complex, *Science* 330 (2010) 974–980.
- [4] G. Kadamur, E.M. Ross, Mammalian phospholipase C, *Annu. Rev. Physiol.* 75 (2013) 127–154.
- [5] A.M. Lyon, J.J. Tesmer, Structural insights into phospholipase C-beta function, *Mol. Pharmacol.* 84 (2013) 488–500.
- [6] T.M. Filtz, D.R. Grubb, T.J. McLeod-Dryden, J. Luo, E.A. Woodcock, G_q -initiated cardiomyocyte hypertrophy is mediated by phospholipase C β 1b, *FASEB J.* 23 (2009) 3564–3570.
- [7] D.R. Grubb, B. Crook, Y. Ma, J. Luo, H.W. Qian, X.M. Gao, H. Kiriazis, X.J. Du, P. Gregorevic, E.A. Woodcock, The atypical 'b' splice variant of phospholipase C β 1a promotes cardiac contractile dysfunction, *J. Mol. Cell. Cardiol.* 84 (2015) 95–103.
- [8] M.R. Dent, N.S. Dhalla, P.S. Tappia, Phospholipase C gene expression, protein content, and activities in cardiac hypertrophy and heart failure due to volume overload, *Am. J. Physiol. Heart Circ. Physiol.* 287 (2004) H719–H727.
- [9] A. Gresset, J. Sondek, T.K. Harden, The phospholipase C isozymes and their regulation, *Subcell. Biochem.* 58 (2012) 61–94.
- [10] W. Zhang, E.J. Neer, Reassembly of phospholipase C- β 2 from separated domains: analysis of basal and G protein-stimulated activities, *J. Biol. Chem.* 276 (2001) 2503–2508.
- [11] A.M. Lyon, V.M. Tesmer, V.D. Dhamsania, D.M. Thal, J. Gutierrez, S. Chowdhury, K.C. Suddala, J.K. Northup, J.J. Tesmer, An autoinhibitory helix in the C-terminal region of phospholipase C- β mediates G_{α_q} activation, *Nat. Struct. Mol. Biol.* 18 (2011) 999–1005.
- [12] C.G. Kim, D. Park, S.G. Rhee, The role of carboxyl-terminal basic amino acids in G_{α_q} -dependent activation, particulate association, and nuclear localization of phospholipase C- β 1, *J. Biol. Chem.* 271 (1996) 21187–21192.
- [13] O. Ilkaeva, L.N. Kinch, R.H. Paulsen, E.M. Ross, Mutations in the carboxyl-terminal domain of phospholipase C β 1 delineate the dimer interface and a potential G_{α_q} interaction site, *J. Biol. Chem.* 277 (2002) 4294–4300.
- [14] A.M. Lyon, S. Dutta, C.A. Boguth, G. Skiniotis, J.J. Tesmer, Full-length Galpha(q)-phospholipase C-beta3 structure reveals interfaces of the C-terminal coiled-coil domain, *Nat. Struct. Mol. Biol.* 20 (2013) 355–362.
- [15] A.U. Singer, G.L. Waldo, T.K. Harden, J. Sondek, A unique fold of phospholipase C- β mediates dimerization and interaction with G_{α_q} , *Nat. Struct. Biol.* 9 (2002) 32–36.
- [16] T.H. Charpentier, G.L. Waldo, M.O. Barrett, W. Huang, Q. Zhang, T.K. Harden, J. Sondek, Membrane-induced allosteric control of phospholipase C-beta isozymes, *J. Biol. Chem.* 289 (2014) 29545–29557.
- [17] S.N. Hicks, M.R. Jezyk, S. Gershburg, J.P. Seifert, T.K. Harden, J. Sondek, General and versatile autoinhibition of PLC isozymes, *Mol. Cell* 31 (2008) 383–394.
- [18] A.M. Lyon, J.A. Begley, T.D. Manett, J.J. Tesmer, Molecular mechanisms of phospholipase C beta3 autoinhibition, *Structure* 22 (2014) 1844–1854.
- [19] B.N. Hudson, S.H. Hyun, D.H. Thompson, A.M. Lyon, Phospholipase Cbeta3 membrane adsorption and activation are regulated by its C-terminal domains and phosphatidylinositol 4,5-bisphosphate, *Biochemistry* 56 (2017) 5604–5614.
- [20] M.J. Adjobo-Hermans, K.C. Crosby, M. Putyrski, A. Bhageloe, L. van Weeren, C. Schultz, J. Goedhart, T.W. Gadella Jr., PLC β isoforms differ in their subcellular location and their CT-domain dependent interaction with G_{α_q} , *Cell. Signal.* 25 (2013) 255–263.
- [21] M.J. Adjobo-Hermans, J. Goedhart, T.W. Gadella Jr., Regulation of PLC β 1a membrane anchoring by its substrate phosphatidylinositol (4,5)-bisphosphate, *J. Cell Sci.* 121 (2008) 3770–3777.
- [22] M. Ghosh, A.V. Smrcka, Assay for G protein-dependent activation of phospholipase C β using purified protein components, *Methods Mol. Biol.* 237 (2004) 67–75.
- [23] E.E. Garland-Kuntz, F.S. Vago, M. Sieng, M. Van Camp, S. Chakravarthy, A. Blaine, C. Corpstein, W. Jiang, A.M. Lyon, Direct observation of conformational dynamics of the PH domain in phospholipases C and beta may contribute to subfamily-specific roles in regulation, *J. Biol. Chem.* 293 (2018) 17477–17490.
- [24] T.M. Mezzasalma, J.K. Kranz, W. Chan, G.T. Struble, C. Schalk-Hihi, I.C. Deckman, B.A. Springer, M.J. Todd, Enhancing recombinant protein quality and yield by protein stability profiling, *J. Biomol. Screen.* 12 (2007) 418–428.
- [25] M.V. Ellis, S.R. James, O. Perisic, C.P. Downes, R.L. Williams, M. Katan, Catalytic domain of phosphoinositide-specific phospholipase C (PLC). Mutational analysis of residues within the active site and hydrophobic ridge of PLC δ 1, *J. Biol. Chem.* 273 (1998) 11650–11659.
- [26] E. Trinquet, M. Fink, H. Bazin, F. Grillet, F. Maurin, E. Bourrier, H. Ansanay, C. Leroy, A. Michaud, T. Durroux, D. Maurel, F. Malhaire, C. Goudet, J.P. Pin, M. Naval, O. Hernout, F. Chretien, Y. Chapleur, G. Mathis, D-myo-inositol 1-phosphate as a surrogate of D-myo-inositol 1,4,5-tris phosphate to monitor G protein-coupled receptor activation, *Anal. Biochem.* 358 (2006) 126–135.
- [27] S.H. Ryu, P.G. Suh, K.S. Cho, K.Y. Lee, S.G. Rhee, Bovine brain cytosol contains three immunologically distinct forms of inositolphospholipid-specific phospholipase C, *Proc. Natl. Acad. Sci. U. S. A.* 84 (1987) 6649–6653.
- [28] A. Glukhova, V. Hinkovska-Galcheva, R. Kelly, A. Abe, J.A. Shayman, J.J. Tesmer, Structure and function of lysosomal phospholipase A2 and lecithin:cholesterol acyltransferase, *Nat. Commun.* 6 (2015) 6250.
- [29] M. Nomikos, A. Mulgrew-Nesbitt, P. Pallavi, G. Mihalyne, I. Zaitseva, K. Swann, A.M. Lai, D. Murray, S. McLaughlin, Binding of phosphoinositide-specific phospholipase C-zeta (PLC-zeta) to phospholipid membranes: potential role of an unstructured cluster of basic residues, *J. Biol. Chem.* 282 (2007) 16644–16653.
- [30] H.J. Hwang, H.J. Jang, L. Cocco, P.G. Suh, The regulation of insulin secretion via phosphoinositide-specific phospholipase Cbeta signaling, *Adv. Biol. Regul.* 71 (2019) 10–18.
- [31] L.H. Xie, M. Horie, M. Takano, Phospholipase C-linked receptors regulate the ATP-sensitive potassium channel by means of phosphatidylinositol 4,5-bisphosphate metabolism, *Proc. Natl. Acad. Sci. U. S. A.* 96 (1999) 15292–15297.
- [32] M.K. Crowder, C.D. Seacrist, R.D. Blind, Phospholipid regulation of the nuclear receptor superfamily, *Adv. Biol. Regul.* 63 (2017) 6–14.
- [33] L. Cocco, M.Y. Follo, I. Faenza, A.M. Billi, G. Ramazzotti, A.M. Martelli, L. Manzoli, G. Weber, Inositolide signaling in the nucleus: from physiology to pathology, *Adv. Enzym. Regul.* 50 (2010) 2–11.
- [34] R. Fiume, W.J. Keune, I. Faenza, Y. Bultsma, G. Ramazzotti, D.R. Jones, A.M. Martelli, L. Somner, M.Y. Follo, N. Divecha, L. Cocco, Nuclear phosphoinositides: location, regulation and function, *Subcell. Biochem.* 59 (2012) 335–361.
- [35] R.G. Jacobsen, F. Mazloumi Gavani, A.J. Edson, M. Goris, A. Altankhuyag, A.E. Lewis, Polyphosphoinositides in the nucleus: roadmap of their effectors and mechanisms of interaction, *Adv. Biol. Regul.* 72 (2019) 7–21.
- [36] R. Fiume, G. Ramazzotti, I. Faenza, M. Piazzi, A. Bavelloni, A.M. Billi, L. Cocco, Nuclear PLCs affect insulin secretion by targeting PPARgamma in pancreatic beta cells, *FASEB J.* 26 (2012) 203–210.
- [37] D. Gupta, T. Kono, C. Evans-Molina, The role of peroxisome proliferator-activated receptor gamma in pancreatic beta cell function and survival: therapeutic implications for the treatment of type 2 diabetes mellitus, *Diabetes Obes. Metab.* 12 (2010) 1036–1047.
- [38] M.A. Hermida, J. Dinesh Kumar, N.R. Leslie, GSK3 and its interactions with the PI3K/AKT/mTOR signalling network, *Adv. Biol. Regul.* 65 (2017) 5–15.
- [39] J.Y. Zhang, D.M. Kowal, S.P. Nawoschik, J. Dunlop, M.H. Pausch, R. Peri, Development of an improved IP(1) assay for the characterization of 5-HT(2C) receptor ligands, *Assay Drug Dev. Technol.* 8 (2010) 106–113.
- [40] C.A. Nash, L.M. Brown, S. Malik, X. Cheng, A.V. Smrcka, Compartmentalized cyclic nucleotides have opposing effects on regulation of hypertrophic phospholipase Cepsilon signaling in cardiac myocytes, *J. Mol. Cell. Cardiol.* 121 (2018) 51–59.
- [41] L. Zhang, S. Malik, J. Pang, H. Wang, K.M. Park, D.I. Yule, B.C. Blaxall, A.V. Smrcka, Phospholipase epsilon hydrolyzes perinuclear phosphatidylinositol 4-phosphate to regulate cardiac hypertrophy, *Cell* 153 (2013) 216–227.